

R

SMITHSONIAN INSTITUTION  
ASTROPHYSICAL OBSERVATORY

Research in Space Science

SPECIAL REPORT

Number 191

OBSERVATION OF THE GT-5 ROCKET-BODY REENTRY —

PRELIMINARY ANALYSIS GPO PRICE \$ \_\_\_\_\_

CFSTI PRICE(S) \$ \_\_\_\_\_

by

Hard copy (HC) 2.00

Leonard H. Solomon

Microfiche (MF) .50

N 66 13768

ff 653 July 65

FACILITY FORM 602

(ACCESSION NUMBER)  
34  
(PAGES)  
CR 68699  
(NASA CR OR TMX OR AD NUMBER)

(THRU)  
1  
(CODE)  
31  
(CATEGORY)

October 22, 1965

CAMBRIDGE, MASSACHUSETTS 02138

CR 68699

SAO Special Report No. 191

OBSERVATION OF THE GT-5 ROCKET-BODY REENTRY —  
PRELIMINARY ANALYSIS

by

Leonard H. Solomon

Smithsonian Institution  
Astrophysical Observatory  
Cambridge, Massachusetts 02138

## TABLE OF CONTENTS

Introduction	1
Data	3
Conclusion	8
Acknowledgments	9
References	9
Appendix 1A	10
Appendix 1B	13
Appendix 2	14
Appendix 3	16
Figures	17
Tables	29

# OBSERVATIONS OF THE GT-5 ROCKET-BODY REENTRY - PRELIMINARY ANALYSIS<sup>1</sup>

by

Leonard H. Solomon<sup>2</sup>

## Introduction

The Gemini 5 capsule was placed in orbit by a Martin Titan 2 booster. This is a two-stage rocket, whose first stage falls to earth. In the case of GT-5, the second stage obtained earth orbit, after which the capsule was separated from it and given an additional velocity increment to produce its desired orbit (Aviation Week and Space Technology, 1965). The second-stage case, a cylinder 10 feet in diameter and 27 feet long, possibly contained some residual liquid fuel; it was tracked by sensors of the NORAD tracking network.

The lifetime of the object in orbit was estimated by NORAD sufficiently early to prepare for observations of decay. NORAD-prepared predictions for Smithsonian stations were used by the observers to prepare a local search program at each site.

From these predictions, the Baker-Nunn camera (Henize, 1957) at Olifantsfontein, South Africa, and a nearby Moonwatch station at Pretoria obtained observations at about 16<sup>h</sup>33<sup>m</sup> UT, 24 August. The observers submitted reports covering station activity during the observations, including visual impressions. These reports are included in their entirety as Appendix 1. Certain questions and answers are also attached.

---

<sup>1</sup>This work was supported by Grants Nos. NsG 87-60 and NsG 563 by the National Aeronautics and Space Administration.

<sup>2</sup>Astronomer, Smithsonian Astrophysical Observatory.



The Moonwatch report included one observation of position and time made by locating the object in a known star field at a time calibrated against a radio time standard. Estimated accuracy of these data is 0.5 degree in position and 0.5 second in time. The Baker-Nunn film eventually yielded for orbit analysis 8 measurements of the brightest fragment, each accurate to about 1 minute of arc in position (Solomon, 1965) and 0.1 second in time. These measurements were made by direct comparison of film and film-scale star charts.

The Baker-Nunn film may also yield some photometric data on cloud-like phenomena apparently associated with the object. Unfortunately, no sensito-metric data accompany this film, so absolute intensity measures are not possible.

Although the film clearly shows that the object had fragmented prior to its acquisition by the Baker-Nunn camera, the film may be useful in a further detailed analysis of the breakup. In particular, precision position measures may be possible. Reproductions of all pertinent frames are given in Figures 1 and 2.

We present in this report certain basic information derived from the SAO data and from available NORAD radar observations. Hopefully, this information can be used to explain consistently all the observed phenomena, and also used in any future analysis of the vehicle fragmentation itself.

The data we considered to have possible value in later analysis were: the time of breakup, the object's height, the trajectory of the main mass, the relation of the object to the earth's shadow, and the intersection of the trajectory with the ground. The associated cloud is certainly of interest. We added other items to this list as they presented themselves in various discussions at the Observatory.

## Data

### 1. Time of breakup

a. The report from Mr. Jack Bennett, Pretoria Moonwatch, states in effect that the fragmentation occurred after  $16^{\text{h}}33^{\text{m}}04^{\text{s}}$  UT, based on naked-eye observations. With telescopic aid fragmentation appeared to continue for a short time.

b. When first recorded by the Baker-Nunn at  $16^{\text{h}}33^{\text{m}}08^{\text{s}}$  the objects had already separated and were rapidly diverging. A number of fragments are visible on each of the eight Baker-Nunn frames. Mr. P. J. Kokaras obtained positions of these and plotted locations relative to the brightest object in Figure 3. The best-fit curves have been extended to intersect the center line, and we note that the intersections are spread out, indicating a gradual breakup. Kokaras estimated the earliest time as  $16^{\text{h}}32^{\text{m}}52^{\text{s}}$ , with clumping of the intersections near  $16^{\text{h}}32^{\text{m}}56^{\text{s}}$  and especially between  $16^{\text{h}}32^{\text{m}}58^{\text{s}}$  and  $16^{\text{h}}33^{\text{m}}00^{\text{s}}$ . The position of the stationary cloud observed near Venus is consistent with the satellite position at about the time of major fragmentation. Of course, the extrapolation is extreme in this case.

### 2. Number of objects

Kokaras has counted 58 objects on the original negative of the frame taken at  $16^{\text{h}}33^{\text{m}}16^{\text{s}}$  UT. More than 40 fragments are visible on each of at least 6 frames.

### 3. Height of explosion

We have computed the height of the cluster of objects by three independent methods, as this is the most important quantity determined. From these calculations we also obtain the trajectory in the rotating geocentric (RG) system and its relation to the observing stations. The RG system is defined ( $X$  = Greenwich,  $Y = 90^\circ$  E longitude,  $Z$  = North Pole, origin, at center of earth). The methods and results are as follows:

a. Direct triangulation. Descriptively, by forward extrapolation of the Baker-Nunn measurements we formed a "simultaneous" observation pair from the two stations. Accuracy of the Baker-Nunn extrapolated position is estimated as  $\sim \pm 0.5$  degree. The observed directions in space are skew lines that almost meet. The midpoint of the shortest line joining them forms a triangle with the stations, and we solved this triangle using a computer program supplied by Mrs. N. Simon. The distance between the direction lines was 2.4 km, and the computed height above the surface is about 110 km at this instant. To estimate the possible errors in this calculation, we assumed the maximum reasonable measurement errors, and found a minimum height of  $\sim 86$  km.

b. Intersection of orbit plane and observed directions. Although an orbit for this object was difficult to derive, because of the great effects of air drag and the scarcity of observations, an accurate orbit plane is rather easily found. The equation of this plane for the time of observation was found in the RG system by use of the right ascension of the ascending node  $\Omega$ , sidereal time at Greenwich  $\theta_G$ , and inclination  $i$  (see Appendix 2). Each line (station-satellite) was also placed in the RG system, and coordinates ( $X, Y, Z$ ) of the intersections were found. Heights are then easily determined. A point of great interest is that the height appeared roughly constant at approximately 108 km; hence the object was still moving parallel to the earth's surface at this time.

c. Direct calculation from the orbit. Mrs. E. Mann and Mrs. B. Miller of the SAO Data Division were able to derive an orbit for this satellite from NORAD radar data using the DØI program (Gaposchkin, 1964). They improved this orbit to include the Baker-Nunn positions, and obtained a final orbit covering the last 2.5 revolutions, which fits 46 observed points. A representative early orbit and the final orbit are found in Appendix 3. Finally, this orbit was used in the program Ephemeris 0 (Joughin, 1963), which gives heights explicitly for specified times.

All results of methods a, b, and c are given in Table 1.

#### 4. Geometrical configuration of stations and vehicle

The range of the satellite from the stations is easily computed from the height and observed  $\alpha$ ,  $\delta$ . A drawing of the configuration is given in Figure 4.

#### 5. Height of earth's shadow

The illumination of the vehicle is important. Is it sunlit or self-luminous? At the latitude and longitude of the satellite at the instant of the Moonwatch observation, sunset occurred at the earth's surface at  $\sim 17^{\text{h}}45^{\text{m}}$  local time. At local time  $18^{\text{h}}24^{\text{m}}32^{\text{s}}$  (time of observation) the subsatellite point was  $39^{\text{m}}32^{\text{s}}$ , or  $\sim 9^{\circ}9'$  into shadow. The solar depression is given by

$$\cos D = \frac{R}{R + h} \quad ,$$

and

$$h = \frac{6374.3}{0.9851} - 6374.3 = 96.4 \text{ km} \quad .$$

Therefore, since the satellite is moving approximately west to east, it is sunlit throughout the period of SAO observation. The clouds seen visually and on the film were almost certainly sunlit. Shadow entry was probably gradual, and the long visibility reported by Kirchhoff and Van't Sant may have been aided by some portions being heated to incandescence. Kokaras, after careful study of the satellite images, also feels that the object must have been sunlit throughout.

#### 6. Location of impact point

From the height values in Table 1 we feel it unwise to attempt at this time any estimate of the time or position at which this body impacted the earth's surface.

#### 7. Velocity of object

Knowing the RG coordinates of the object at nine different times, we can calculate the space velocity directly by  $V = \frac{P_2 - P_1}{\Delta T}$ . The mean of the 8 velocities in Table 2 is 8.1 km/second. We see no tendency toward systematic change in the velocity in this short time. This velocity is about as expected for a body reentering the atmosphere from circular orbit (McCrosky, 1965). Approximate values of velocity derived from observed angular velocities are similar to those computed directly.

#### 8. Expansion of the fragments

From the approximate angular separations of the outer fragments, given their ranges, we have computed the projected velocity relative to the main body,  $V = V' \sin i$ , where  $V'$  is the true velocity and  $i$  the unknown angle between line of flight and line of sight;  $V$  is therefore a minimum value. The calculation is shown schematically with results in Table 3. More precise values can be obtained by using the data in Figure 3; however, the speed of separation of the outer fragments is at least of the order of 120 m/second.

## 9. The clouds

Expansion and dissipation of the following cloud is visible within the 16 seconds covered by photography. Film quality is good, and this effect seems to be real. At  $16^{\text{h}}33^{\text{m}}12.0^{\text{s}}$  the cloud has approximate dimensions 2.6 km (perpendicular to direction of motion)  $\times$  52.4 km (along direction of motion), assuming it has expanded into a circular cylindrical shape.

The stationary cloud maintained its integrity for at least 4 minutes, as reported by both observers. The main cloud's size is roughly 3.4 km  $\times$  37.5 km, with a long extension disappearing about 69 km in the direction of motion, all measured on the exposure taken at  $16^{\text{h}}34^{\text{m}}33.7^{\text{s}}$ .

This cloud does not resemble a natural meteor train. Figure 5 is an enlargement of a Baker-Nunn film of one such trail photographed at the Spain tracking station. It shows a distortion due to high-altitude winds. The circumstances are described in a teletype message from the station as follows:

minus 4-5 magnitude white meteor seen THISTA  
at 17/05/17Z. Train smoke photographed (film  
SC 04-16348) 10 degrees long lasted 7 minutes.  
Object fell vertically disappearing above  
horizon near Alkaid.

Further study by Kokaras showed that this was probably a Leonid meteor and could not be a reentering satellite.

We present, in Figure 6, for additional comparison, a reproduction of a Baker-Nunn photograph of a cloud that is presumably the result of propellant venting by an Atlas rocket. This was photographed at the Maui station on 10 June 1965. We consider it likely that the regular pattern of this cloud is maintained because of this vehicle's higher altitude and lower velocity than that of the GT-5 rocket.

## Conclusion

The SAO tracking stations acquired, tracked, and provided useful descriptive information of the GT-5 second-stage reentry, based on NORAD predictions. The height of the object and the velocity of separation of the fragments suggest that the breakup was not strictly analogous to meteor fragmentation. We feel instead that the observations must somehow be explained on the basis of interaction between the vehicle subsystems and the environment. Contributing factors may have been atmospheric friction or shock (although the latter should be small), the presence of residual fuel, spin rate due to unsymmetrical venting of residual fuel, or possibly any pyrotechnics left on board.

One possible explanation evolved in our discussions at SAO is as follows: The body, containing some residual fuel and probably spinning, began to react with increasingly dense atmosphere during its final revolutions. In particular this effect would be largest in the diurnal atmospheric bulge, from which the satellite was probably emerging just prior to the South Africa passage. Some areas of the vehicle, particularly the leading edges, could become heated to incandescence and commence fragmenting. Supposing some liquids remained in the tanks, if the early fragmentation reached a weak point in the walls or tubing, a rapid depressurization or possibly an explosion occurred, producing the brilliant flash and a cloud. This cloud of gas was decelerated by the atmosphere to become the observed stationary object. A continuing outflow of gas would produce the trailing cloud. Smoke produced by burning of the destruct system might be similarly acted upon, and activation of the destruct system would also have fragmented the vehicle.

The rapid decompression of residual liquid could produce the observed transverse fragment velocities, which are almost an order of magnitude above the 15 to 20 m/second estimated for meteor fragmentation (McCrosky, 1965). Explosion of the rocket's automatic destruct system might also produce the observed velocities. Transverse velocities would also be increased by spinning of the vehicle prior to fragmentation.

## Acknowledgments

I am grateful for discussions with Drs. L. Jacchia, C.A. Lundquist, and R. E. McCrosky and Messrs. E. M. Gaposchkin, W. Joughin, A. Werner, P. Brand, and W. Hirst. I was assisted in some of the calculations by Mrs. J. Pearlmutter and Miss M. David.

## References

### AVIATION WEEK AND SPACE TECHNOLOGY

1965. Gemini 5 sustains accelerated U.S. pace. Aviation Week and Space Technology, August 30, pp. 24-29.

### GAPHOSCHKIN, E. M.

1964. Differential orbit improvement (DØI-3). Smithsonian Astrophys. Obs. Spec. Rep. 161, August 3.

### HENIZE, K. G.

1957. The Baker-Nunn satellite-tracking camera. Sky and Tel., vol. 16, pp. 108-111.

### JOUGHIN, W.

1963. SAO Ephemeris O. SAO Program Writeup, May.

### MCCROSKY, R. E.

1965. Private communication.

### SOLOMON, L. H.

1965. Residuals in field-reduced observations. Smithsonian Astrophys. Obs. Spec. Rep. 176, May 17, pp. 3-4.



## APPENDIX 1A

### REPORT OF MOONWATCH OBSERVER

#### Reentry of Gemini 5 Booster Rocket

On August 25, 1965 the Gemini 5 rocket was due to pass over Pretoria at  $16^{\text{h}}31^{\text{m}}$  UT. It failed to appear at the expected time. At a little before  $16^{\text{h}}33^{\text{m}}$ , however, an object appeared in the S.S.W. sky. It was a striking object, but not as bright as Venus. It seemed to be glowing dully and floating upwards. As soon as I realized that it was the rocket, I pressed my first stop-watch (time ascertained later:  $16^{\text{h}}33^{\text{m}}04^{\text{s}}$ ).

Suddenly the object exploded into a red incandescent globe, nearly the size of the full moon. I sighted the 5" apogee telescope on it and found it to be like the head of a great comet, a glowing core surrounded by a hazy red "coma" with matter streaming back along a brilliant trail. The redness faded out and a cascade of silver sparks began to shoot off the head in all directions. As the rocket broke up, the field of the telescope was filled with about a dozen "satellites" all flying along together. I concentrated on the brightest piece and in spite of the great speed managed to get a stop-watch check quite close to a star which turned out to be Rho Lupi.

With the telescope stopped at this point, I quickly checked the star field and then looked up to find no trace of the rocket in the sky. The smoke trail was fading and broken.

A further careful check of the field then followed.

Four minutes after my first stop-watch check, a small puff of white smoke was still visible  $6^{\circ}$  S.S.W. of Venus as measured in the field of my 10 x 60 binoculars. It was about a degree or more in diameter and was apparently the remains of the original explosion.

J. Bennett  
Pretoria, South Africa  
8/25/65

Dear Mr. Hirst:

Thanks for your telex message about my observation of the Gemini 5 rocket.

Will you please make one correction to my report posted yesterday. The rocket first appeared in the W.N.W. sky (not S.S.W.), of course.

I also omitted to say that the rocket started to leave a trail in the sky just before the first explosion. Unfortunately, I do not remember the color of the trail, but it was dark and clearly visible, increasing in width as the rocket hurtled nearer, and then the big explosion took place.

This was the most exciting observation I have ever made.

Best wishes

Jack Bennett

8/26/65

TO JACK BENNETT PRETORIA MOONWATCH

REFERENCE GT-5 ROCKET REENTRY REPORT. ANALYSIS OF B-N FILM RAISED FOLLOWING QUESTIONS.

1. WHAT TIME STANDARD WAS USED FOR CALIBRATING FIRST STOPWATCH TIME.
2. ESTIMATE INTERVAL BETWEEN 16:33:04 AND OBSERVED EXPLOSION.
3. ESTIMATE INTERVAL DURING WHICH RED GLOBE EXISTED.
4. ESTIMATE LARGEST POSSIBLE ERROR IN TIME AND POSITION REPORTED.
5. WERE THERE ANY HIGH CLOUDS IN AREA OTHER THAN PUFF CREATED BY EXPLOSION.

THIS IS NECESSARY FOR TOTAL EVALUATION OF REENTRY. REQUEST REPLY ASAP VIA THIS CHANNEL. MANY THANKS

FOLLOWING ANSWERS RECEIVED FROM JACK BENNETT

1. FIRST STOPWATCH TIMED AGAINST SECOND TO FREE IT. SECOND TIMED AGAINST Z U O SAME STANDARD USED BY SC O2
2. FOUR TO SIX SECONDS
3. ALSO FOUR TO SIX SECONDS
4. HALF SECOND IN TIME HALF DEGREE IN POSITION
5. NO

FURTHER CORRECTION RECEIVED FROM BENNETT

8/26/65 LETTER CLARIFIED READS DARK TRAIL AGAINST CLEAR SKY

## APPENDIX 1B

### Report of Baker-Nunn Observers

REPORT ON GT5 ROCKET REENTRY AUG 24.

CAMERA OPERATION KIRCHHOFF OBSERVER VANTSANT. SEARCH COMMENCED AT 1620Z. SCATTERED CIRRUS BANDS BETWEEN NW HORIZON AND VENUS. SKY BRIGHTNESS LATE TWILIGHT, MAGNITUDE OF FAIINTEST STAR NEAR VENUS PLUS 2.

OBJECT FIRST SEEN 20 DEGREES ALONG TRACK PRIOR TO EXPLOSION AS BRIGHT PEGASUSLIKE SATELLITE SHOWING APPARENT SIGNS OF TUMBLING. FIRST SIGHTING BEING AT PEAK, SECOND PEAK CONTINUED TO GROW RAPIDLY THROUGH BRIGHT WHITEHOT RED TO BRILLIANT WHITE VERYFLARE LIKE FLASH LASTING 3-5 SECONDS 3 DEGREES NW OF VENUS.

THIS FLASH LEFT IMMEDIATE LARGE CLOUD. NO SMOKE PRIOR TO EXPLOSION NOTICED THROUGH CIRRUS. FLASH EMITTED NUMEROUS SPARKS IN ALL DIRECTIONS GIVING FLASH APPARENT DIAMETER AND BRIGHTNESS OF FULL MOON. AFTER FLASH OBJECT APPEARED AS ZERO MAGNITUDE MOVING VERY RAPIDLY WITH IRREGULAR FURTHER MINOR SUDDEN SPARKLIKE FLASHES VISIBLE MAINLY ON BOTH SIDES OF MAIN OBJECT LEAVING OCCASIONAL SMALL CLOUDS OF SHORT DURATION. MAIN OBJECT STILL SEEN 25 DEGR ABOVE SE HORIZON BUT MOST FLASHING HAD CEASED AFTER CROSSING MERIDIAN. NO LONG LASTING TRAIL REMAINED EXCEPT CLOUD OF FIRST EXPLOSION. THIS WAS VISIBLE FOR SEVERAL MINUTES AND PHOTOGRAPHED AFTER END OF MAIN SERIES. TRANSVERSE CLOUD EFFECT ON RIGHTHAND EDGE ON THOSE FRAMES OF EXPLOSION CLOUDS IS CAUSED BY BAND OF CIRRUS. MAIN SERIES PHOTOGRAPHY WAS CONTINUOUS 4 SEC PER CYCLE OPERATION. CAMERA SETTING CHOSEN AT TRACKANGLE 60 TO AVOID CIRRUS IN WEST. AS SOON AS OBJECT WAS SIGHTED CAMERA WAS REVERSE TRACKED FROM T. A. 60 TOWARDS IT. OBJECT ENTERED FIELD WHEN REACHING T.A. 50 AND TRACKING DRIVE STOPPED. FORWARD TRACK STARTED WHEN OBJECT WAS NEARLY THROUGH FIELD BUT AS VELOCITY WAS TWICE THAT OF MAXIMUM OF CAMERA OBJECT COULD NOT BE REACQUIRED. OBJECT HAD DISAPPEARED BEFORE 90 DEGR AZIMUTH SWING AND ALTITUDE CHANGE COULD BE ACCOMPLISHED.

## APPENDIX 2

### CALCULATION OF OBJECT HEIGHT, USING ORBIT PLANE AND OBSERVED DIRECTIONS

The orbit plane, in RG system, passes through the origin and the ascending node, and is inclined at an angle  $i$  to the plane  $z = 0$ . The direction cosines of its normal are

$$\begin{aligned} a &= \sin i \cos [\Omega - \theta_G - 90^\circ], \\ b &= \sin i \sin [\Omega - \theta_G - 90^\circ], \\ c &= \cos i, \end{aligned}$$

where  $i = 32.61$ ,

$$\Omega = 18.94,$$

$\theta_G$  = Sidereal time at Greenwich meridian.

The plane is then

$$aX + bY + cZ = 0,$$

Direction cosines of the lines from observing station to satellite are given by

$$\begin{aligned} l &= \cos \delta \cos (\alpha - \theta_G), \\ m &= \cos \delta \sin (\alpha - \theta_G), \\ n &= \sin \delta, \end{aligned}$$

where

$\alpha$  = right ascension,

$\delta$  = declination.

The lines are therefore

$$\frac{X - X_s}{l} = \frac{Y - Y_s}{m} = \frac{Z - Z_s}{n},$$

where  $X_s$   $Y_s$   $Z_s$  refer to station coordinates. We solve this system of three equations to obtain

$$Y = \left(\frac{m}{l}\right) X + Y_s - \left(\frac{m}{l}\right) X_s$$

$$Z = \left(\frac{n}{l}\right) X + Z_s - \left(\frac{n}{l}\right) X_s$$

and

$$X = \frac{-b \left[ Y_s + \left(\frac{m}{l}\right) X_s \right] - c \left[ Z_s + \left(\frac{n}{l}\right) X_s \right]}{a + b \left(\frac{m}{l}\right) + c \left(\frac{n}{l}\right)},$$

which are easily solved in practice.

Finally,

$$h = \sqrt{X^2 + Y^2 + Z^2} - R_e ,$$

where  $h$  = height over the surface, and we take

$$R_e = 6374.3 \text{ km} .$$

### APPENDIX 3

#### SATELLITE 1965 68B GEMINI 5 ROCKET

(Prepared by Mrs. E. Mann)

##### SAO smoothed elements

The following elements are based on 74 observations and are valid for the period August 21 through August 23, 1965:

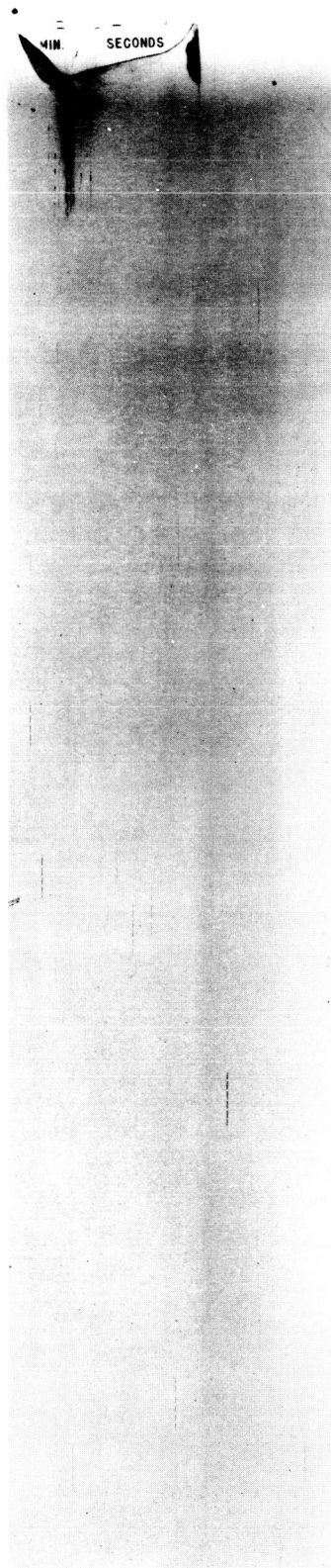
$$\begin{aligned}T_0 &= 38994.0 \text{ MJD} \\ \omega &= 70^\circ.74 + 11^\circ.19832 \text{ t} \\ \Omega &= 38^\circ.9115 - 7^\circ.4030 \text{ t} \\ i &= 32^\circ.5996 \\ e &= .013201 - .002894 \text{ t} \\ M &= .66168 + 16.125585 \text{ t} + .03384 \text{ t}^2 - .00139 \text{ t}^3 + .00186 \text{ t}^4\end{aligned}$$

Standard error of one observation:  $\sigma = \pm 6.70$ .

The following elements are based on 46 observations and are valid for the period August 24.5 through August 24.7, 1965:

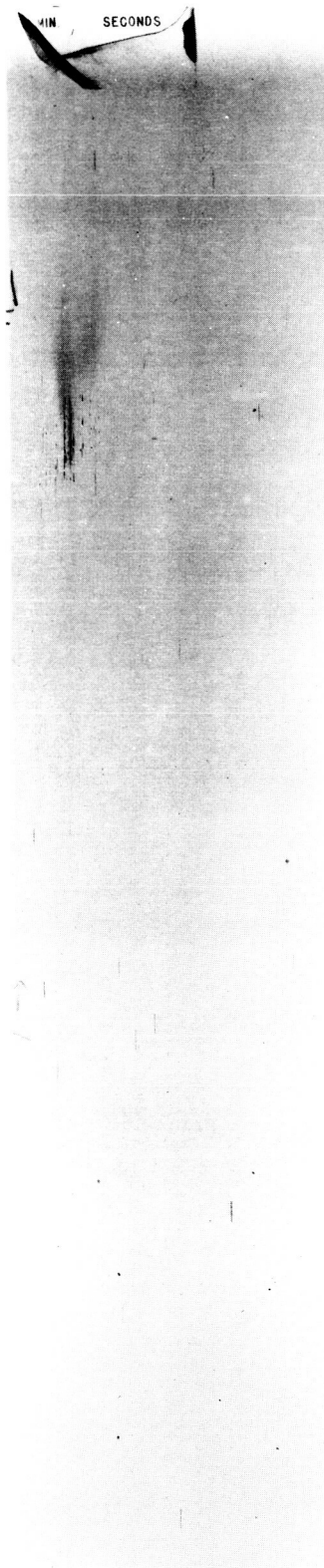
$$\begin{aligned}T_0 &= 38996.5 \text{ MJD} \\ \omega &= 110^\circ.0945 + 12^\circ.0424 \text{ t} \\ \Omega &= 20^\circ.2582 - 7^\circ.8893 \text{ t} \\ i &= 32^\circ.60518 \\ e &= .004253 \\ M &= .214908 + 16.2309 \text{ t} + 3.996 \text{ t}^2 - 30.33 \text{ t}^3 + 81.11 \text{ t}^4\end{aligned}$$

Standard error of one observation:  $\sigma = \pm 1.91$ .



(a)

Time 16<sup>h</sup>33<sup>m</sup>08<sup>s</sup>.00 camera tracking at partial rate, fragments at extreme end of frame.

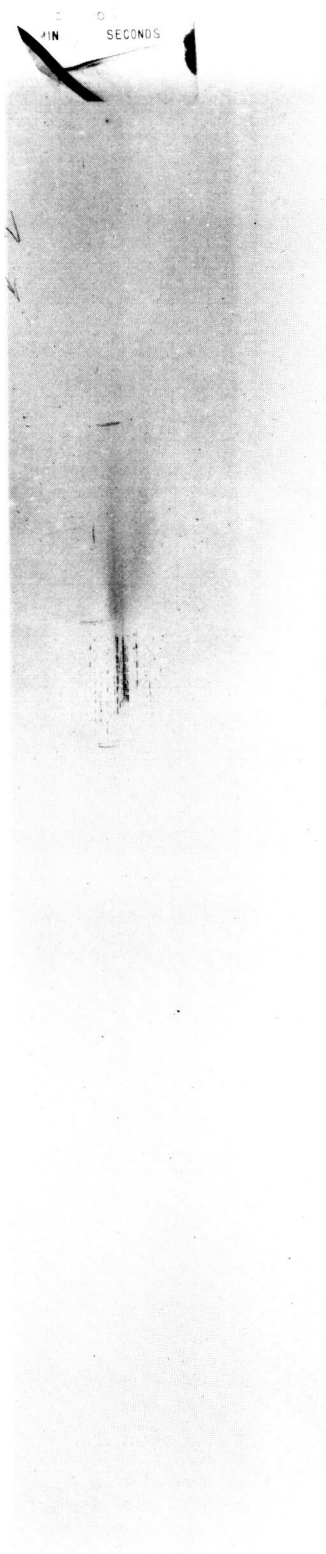


(b)

Time 16<sup>h</sup>33<sup>m</sup>10<sup>s</sup>.00 camera tracking at partial rate. Note heavy, bright cloud split into two sections.

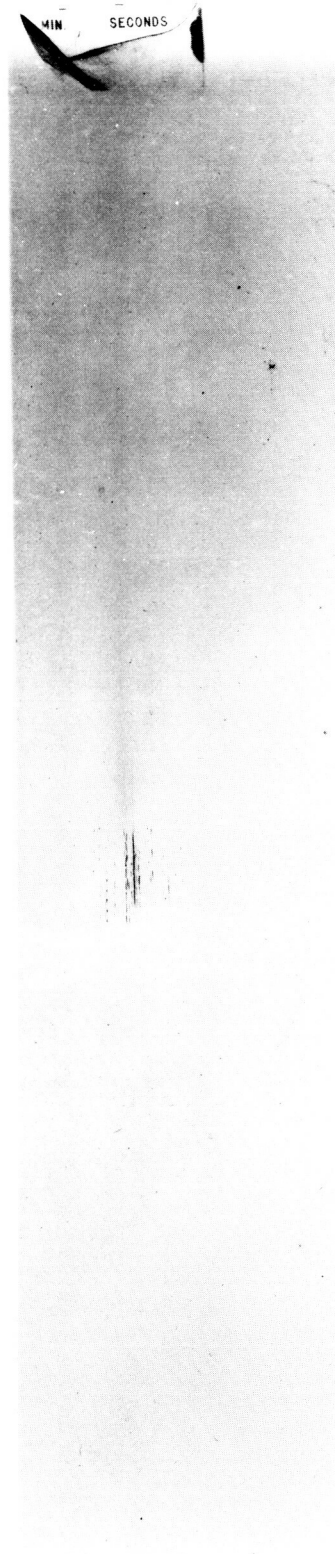
Figure 1.





(c)

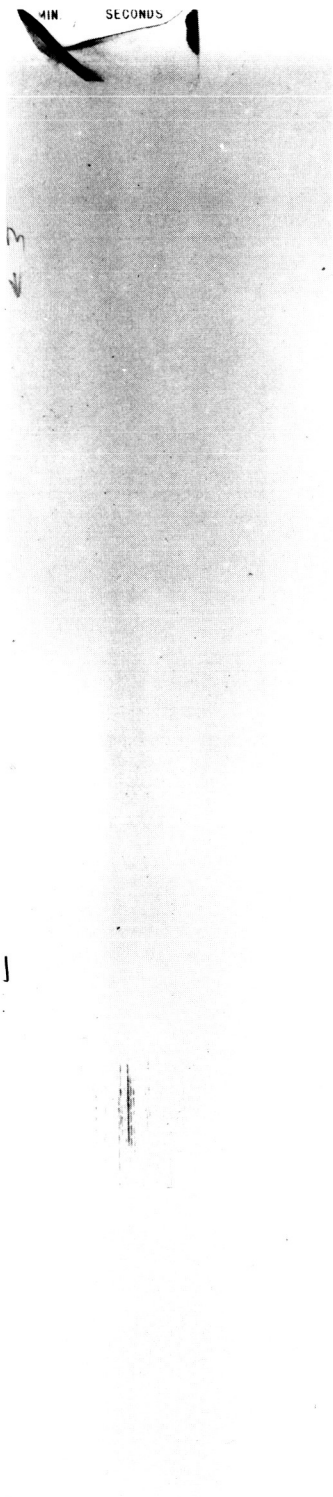
Time 16<sup>h</sup> 33<sup>m</sup> 12.00 camera stationary.



(d)

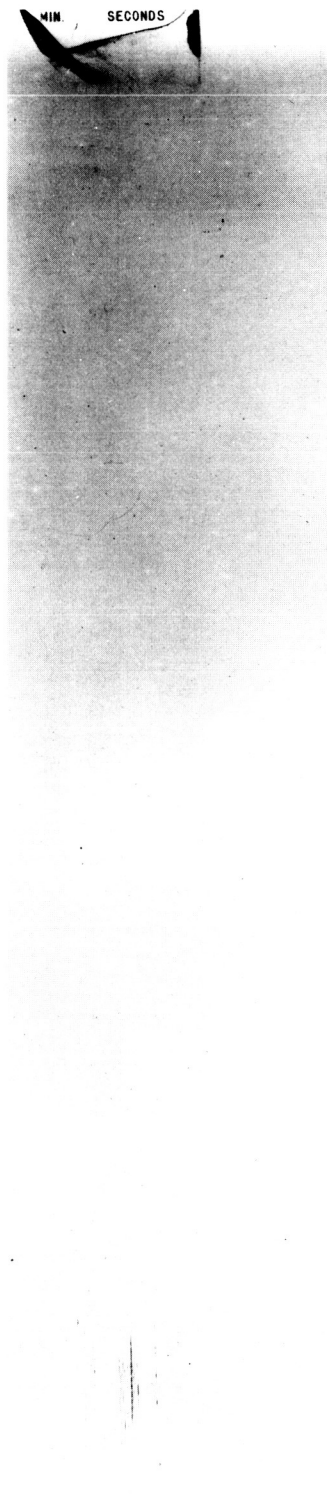
Time 16<sup>h</sup> 33<sup>m</sup> 14.00 camera stationary. Cloud dissipating. The light band is a drying mark.

Figure 1.



(e)

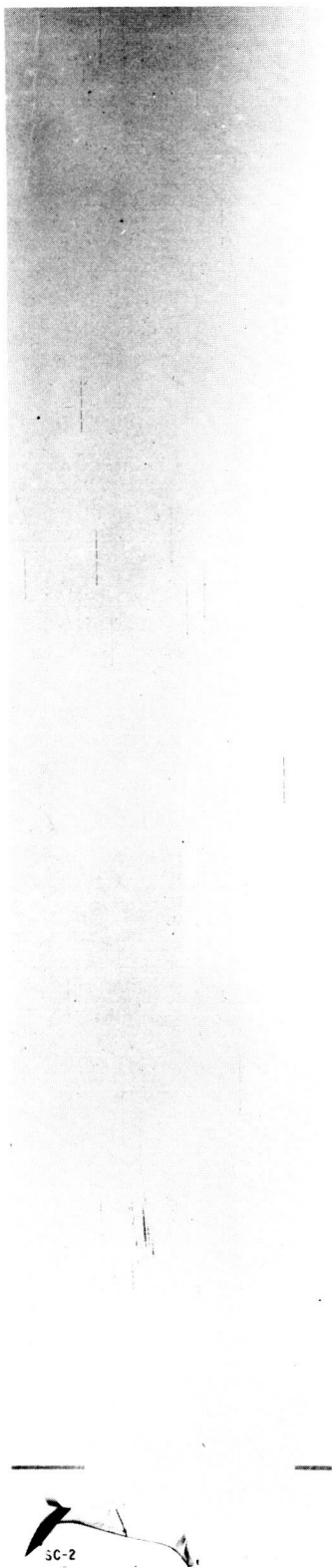
Time 16<sup>h</sup>33<sup>m</sup>16<sup>s</sup>.00 camera stationary. Fifty-eight objects found in original negative.



(f)

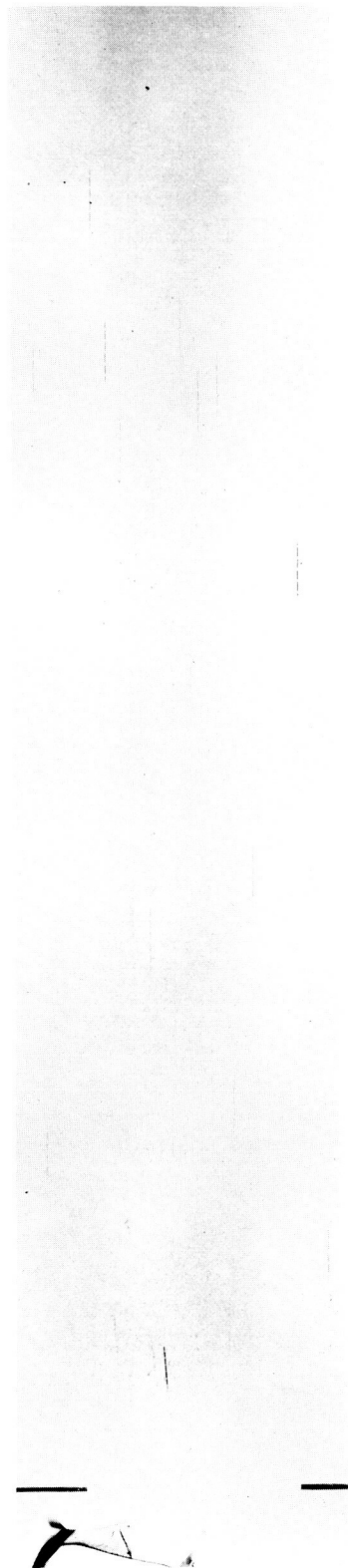
Time 16<sup>h</sup>33<sup>m</sup>18<sup>s</sup>.00 camera stationary.

Figure 1.



(g)

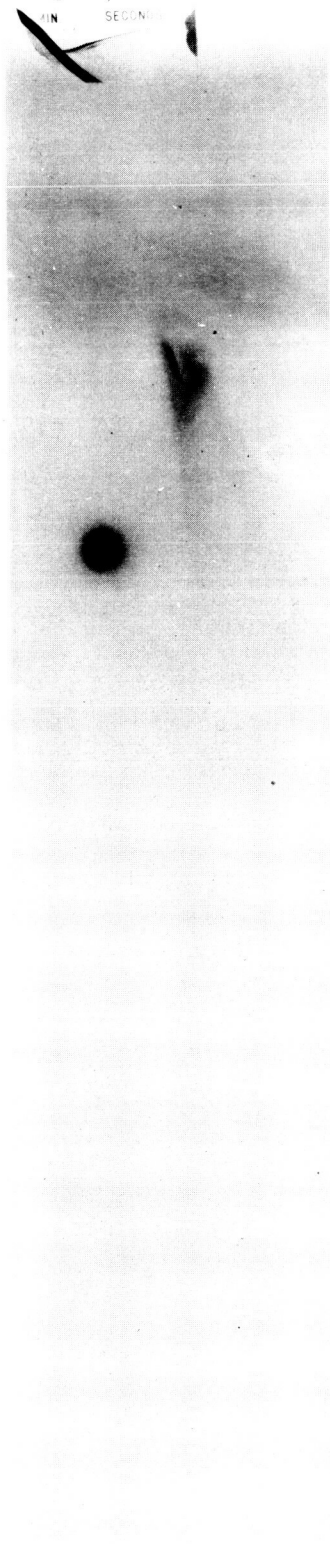
Time 16<sup>h</sup>33<sup>m</sup>20.00 camera tracking at partial velocity.



(h)

Time 16<sup>h</sup>33<sup>m</sup>22.00 camera tracking at partial velocity, fragments at extreme end of frame.

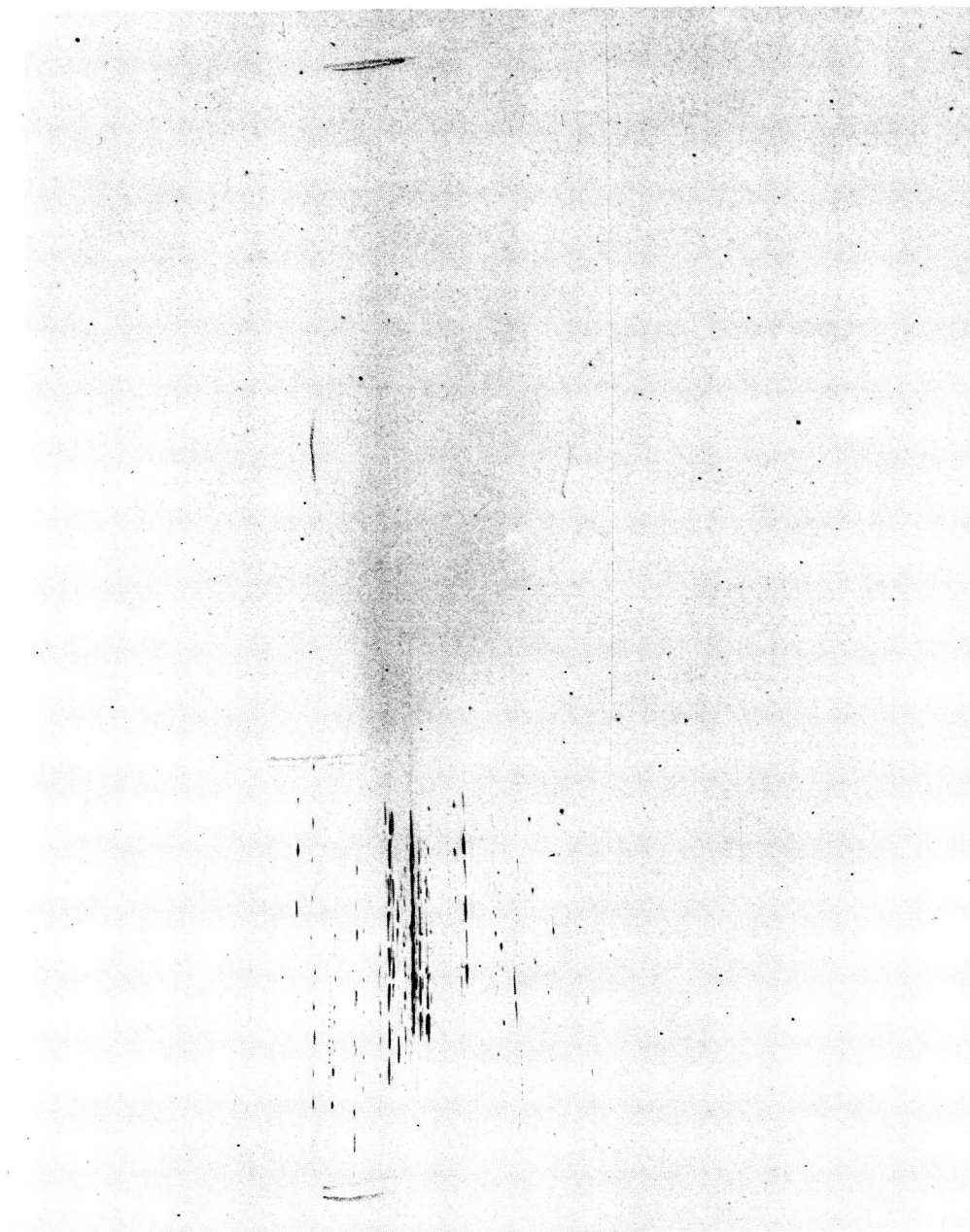
Figure 1.



(1)

Time 16<sup>h</sup>34<sup>m</sup>35 camera stationary.  
Stationary cloud in vicinity of Venus.

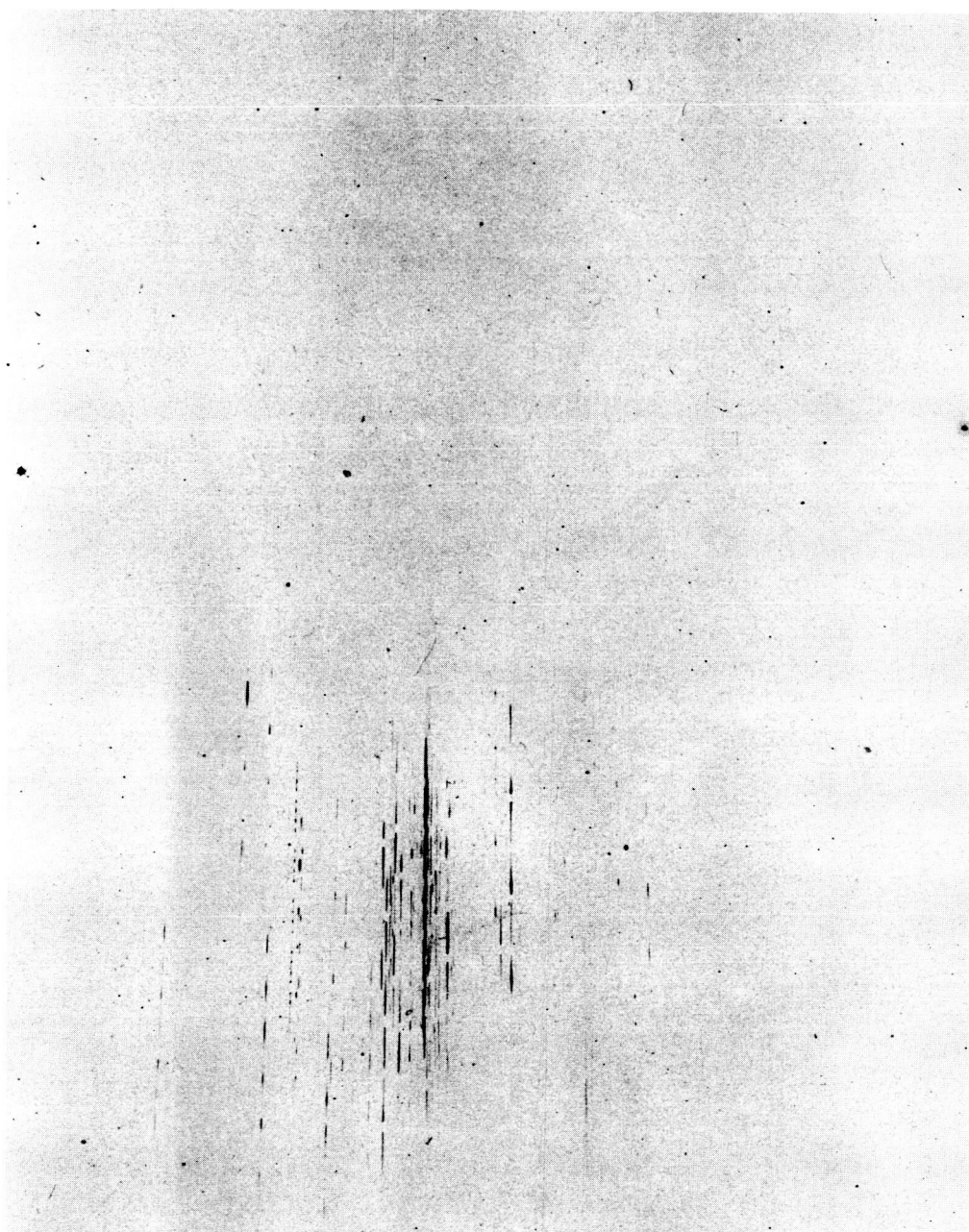
Figure 1.



(a)

Frame 3, enlarged 5 times. Note trailing cloud, brightest near fragments, apparent slow tumbling of some objects, rapid flashing of others. Five shutter breaks are also visible.

Figure 2.

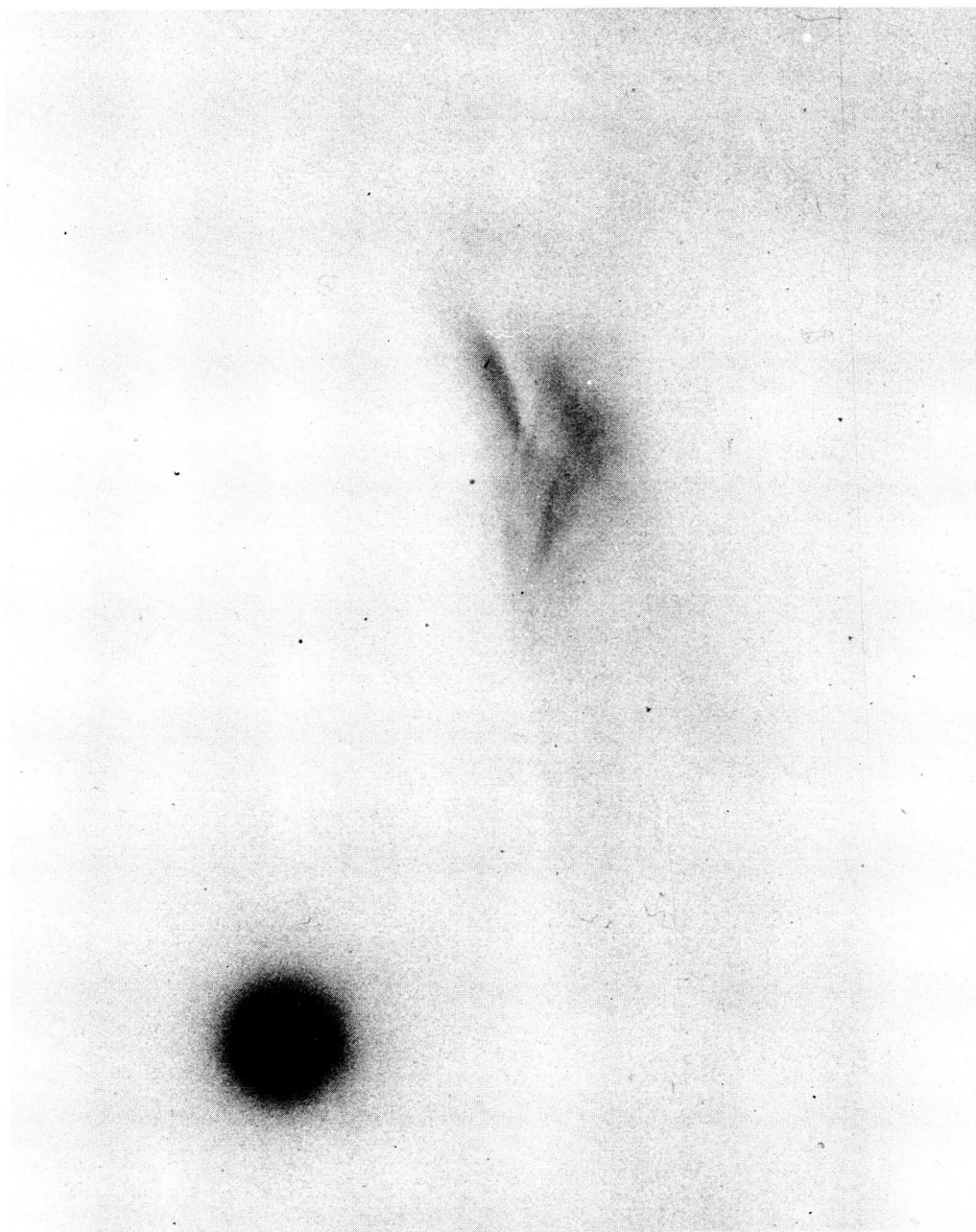


(b)

Frame 6, enlarged 5 times. Note expansion of fragments and apparent dissipation of trailing cloud.

Figure 2.





(c)

Stationary cloud, bright object is Venus. Note smooth undisturbed nature of filamentary structure.

Figure 2.

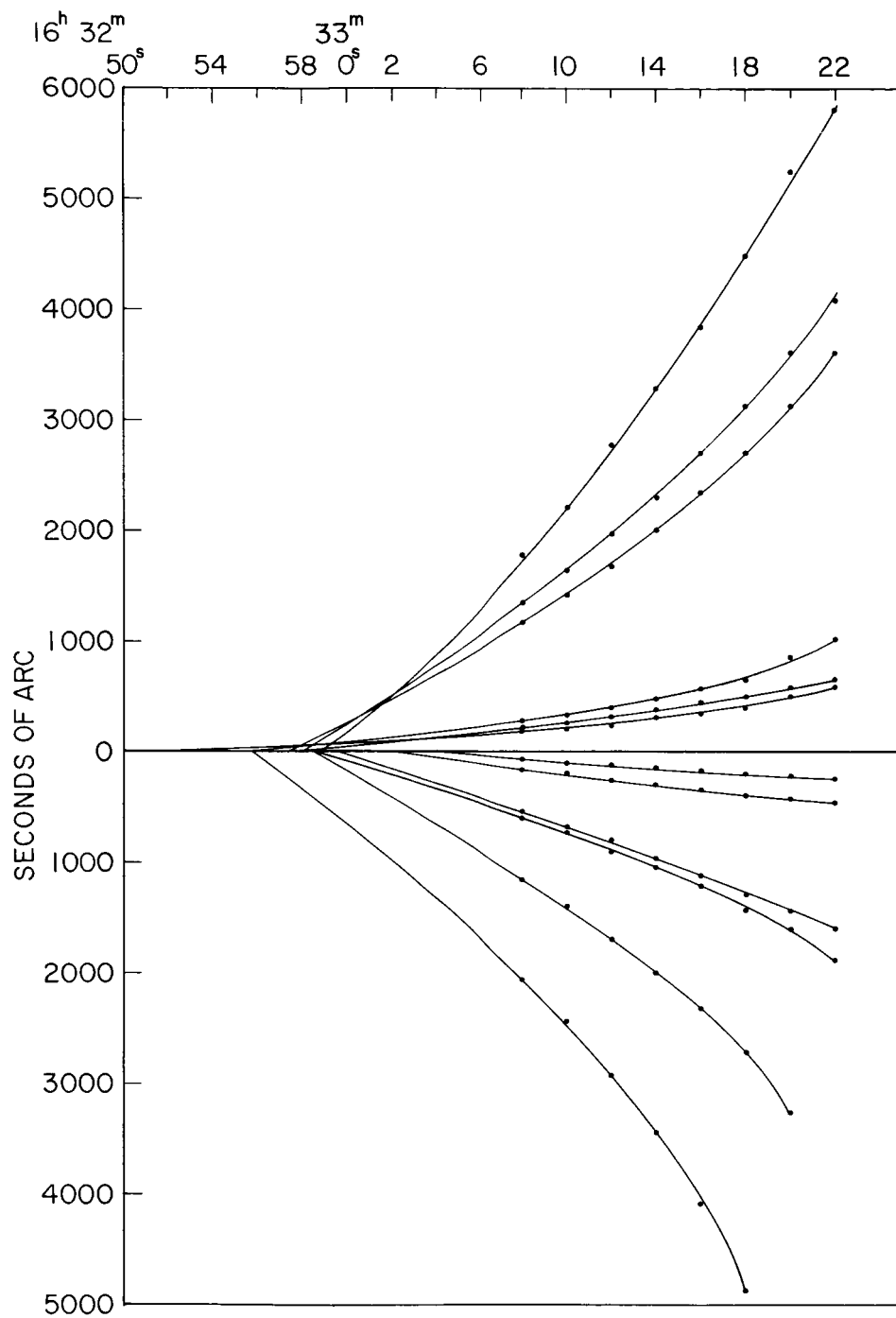


Figure 3.--Apparent expansion of fragments. Relative positions measured from Baker-Nunn film.





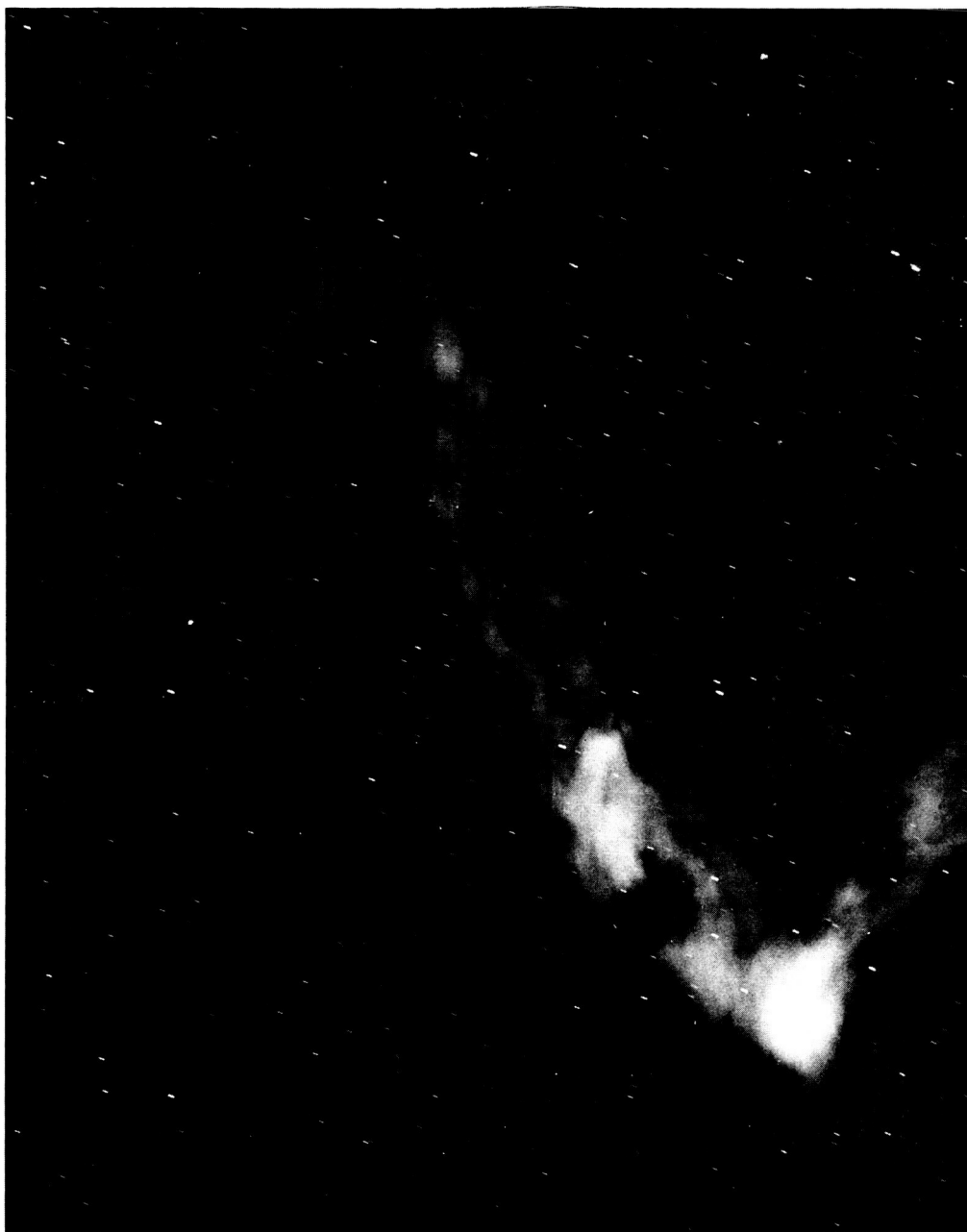


Figure 5.--Natural meteor train observed by Spain Baker-Nunn camera.  
Photographed about 1 minute after meteor passed.



Figure 6.--Aftermath of presumed propellant venting, Atlas Rocket. Photographed  
by Maui Baker-Nunn, 10 June 1965.

Table 1.--Coordinates and heights of the cluster of objects.

Measured Position No.		1	2	3	4	5	6	7	8	9 (B-N)	9 (MW)
<u>Method:</u>											
a	X ( $10^6$ m)	(									
	Y										
	Z	Not Applicable									
	h (km)	)									
		5.15514									
		2.71570									
		-2.85445									
		110.1									
	Minimum distance (km)	2.4									
b	X	5.22708	5.22317	5.20519	5.20162	5.19306	5.18511	5.17624	5.16764	5.15172	5.15183
	Y	2.61125	2.62310	2.63511	2.64696	2.65896	2.67131	2.68328	2.69528	2.71381	2.71320
	Z	-2.80527	-2.81163	-2.81473	-2.82138	-2.82675	-2.83251	-2.83781	-2.84320	-2.85079	-2.84928
	h (km)	107.2	111.5	103.3	108.2	108.6	109.9	110.0	110.5	108.9	108.1
c	h	106.4	106.4	106.4	106.5	106.5	106.5	106.5	106.5	106.6	

Table 2.--Computed space velocity of principal object.

Obs. no. n	1	2	3	4	5	6	7	8	9(M/W)
$V = \frac{P_{n+1} - P_n}{\Delta t}$	7.0	10.9	7.0	7.8	7.9	7.9	7.9	8.2	—

mean 8.1 km/sec

Table 3.--Schematic calculation of fragment-separation velocity .

Time 16 <sup>h</sup> 35 <sup>m</sup> +	Linear extent of fragment group	Angular extent (seconds of arc)	Angular extent (radians)	Range (km)	Linear dispersion (m)	Δ size (m)
12 <sup>s</sup> .0	10.7	4460	0.0216	174	3758	509
14 <sup>s</sup> .0	12.6	5250	0.0254	168	4267	427
16 <sup>s</sup> .0	14.8	6170	0.0299	157	4694	466
18 <sup>s</sup> .0	17.2	7170	0.0348	148	5150	_____

Δ size (mean) 467 m

Δ size/second ≈ 234 m/second

expansion velocity =  $\frac{1}{2}$  Δ size/second ≈ 117 m/second

## NOTICE

This series of Special Reports was instituted under the supervision of Dr. F. L. Whipple, Director of the Astrophysical Observatory of the Smithsonian Institution, shortly after the launching of the first artificial earth satellite on October 4, 1957. Contributions come from the Staff of the Observatory.

First issued to ensure the immediate dissemination of data for satellite tracking, the reports have continued to provide a rapid distribution of catalogs of satellite observations, orbital information, and preliminary results of data analyses prior to formal publication in the appropriate journals. The Reports are also used extensively for the rapid publication of preliminary or special results in other fields of astrophysics.

The Reports are regularly distributed to all institutions participating in the U. S. space research program and to individual scientists who request them from the Publications Division, Distribution Section, Smithsonian Astrophysical Observatory, Cambridge, Massachusetts 02138.